

Self-Assembled Double-Stranded DNA (dsDNA) Microarrays for Protein:dsDNA Screening Using Atomic Force Microscopy

Janese C. O'Brien,[†] John T. Stickney,[‡] and Marc D. Porter^{*‡}

Microanalytical Instrumentation Center
Ames Laboratory-DOE, and Department of Chemistry
Iowa State University, Ames, Iowa 50011
Department of Biochemistry, Biophysics, and
Molecular Biology
Iowa State University, Ames, Iowa 50011

Received February 3, 2000

Revised Manuscript Received March 28, 2000

A novel method for creating and interrogating dsDNA microarrays suitable for screening protein:dsDNA interactions is described. Our strategy combines the ease of self-assembled monolayer technology with the ability of the atomic force microscope (AFM) to detect changes in surface topography at a subnanometer length scale. The methodology involves the direct deposition of double-stranded oligonucleotides (Figure 1A) synthesized by exploiting the high efficiency of off-chip phosphoramidite chemistry to (1) contain asymmetrically substituted disulfide functionalities¹ which direct their self-assembly onto gold in a single step,² (2) include a recognition sequence specific to a given restriction enzyme, (3) position the recognition sequence within the duplex such that enzymatic cleavage results in a topographic change readily detectable by AFM (Figure 1B), and (4) contain a fluorescent tag³ positioned above the recognition sequence to optically verify cleavage. The as-assembled arrays are further modified by exchange with a short chain thiol^{2b} to decrease duplex density. Taken together, these steps form an adlayer in which the spatial orientation and packing density of dsDNA are well suited to function as microarrays for protein screening.

We have adopted a five-step microarray fabrication process that draws on concepts presented in our reports on height-based immunoassays⁴ and on modifications to a strategy for the self-assembly of ssDNA onto gold.⁵ Briefly, step 1 forms a thiol-derived (CF₃(CF₂)₇(CH₂)₂SH) fluorinated monolayer on gold which serves, after photopatterning, as an internal reference plane for the detection of topographic changes; its low surface free energy also minimizes nonspecific adsorption.^{4b} Step 2 is the photopatterning process whereby a metallic grid (hole size: 7.5 μm, grid size: 5.0 μm) acts as a mask. Irradiation of the sample converts the thiolate to oxygenated forms of sulfur that are rinsed off the gold surface with most organic solvents.⁶ Step 3 removes the oxygenated adlayer by rinsing with ethanol to expose square-shaped regions on the underlying gold. Step 4 exposes the

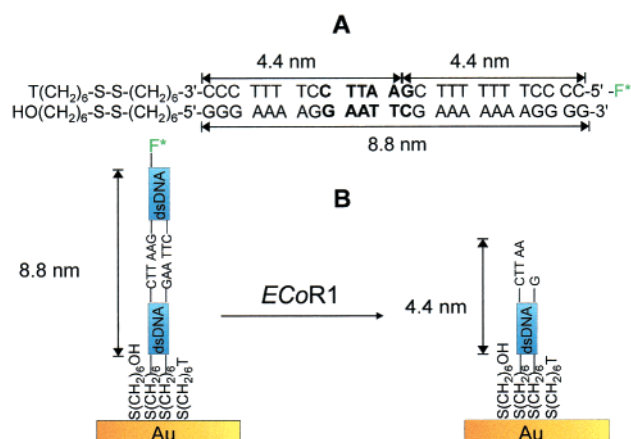


Figure 1. (A) Disulfide-modified double-stranded 26-mer containing the recognition sequence (in bold) specific for *Eco*R1. X-ray crystallography predicts the lengths of 8.8 and 4.4 nm for the intact and cleaved oligonucleotides in their B-conformation,¹¹ respectively. Each 26-mer was labeled with fluorescein (F*) at the 5'-end for use in optical verification of sequence specific cleavage. The "T" on end of the 3'-thiol-modified oligonucleotide was the "dummy base" used to make the 3'-modification. (B) Conceptualized topographic change after exposure of dsDNA microarray to *Eco*R1.

patterned surface to a dsDNA solution⁷ and coats the exposed regions of gold with a mixed monolayer through cleavage of the disulfide linkage^{2,8} attached to both duplex strands (Figure 1A). Step 5 exchanges a portion of immobilized dsDNA with a short chain alkanethiol (i.e., HO(CH₂)₆SH, (MCH)).⁹ This step reduces duplex density, a key factor in increasing enzymatic accessibility to specific recognition sequences within individual addresses (see below).¹⁰

Figures 2 and 3 present in situ AFM topographic images and cross-sectional plots that demonstrate the diagnostic capability of our strategy. Figure 2A shows an image for an array comprised of double-stranded 26-mers containing a recognition sequence specific for the enzyme *Eco*R1 (Figure 1A). The 8.8 ± 1.5 nm (*n*=5) difference in height between grid and square regions agrees with the X-ray crystallographic prediction of 8.8 nm for a double-stranded 26-mer in its B-conformation.¹¹ This result demonstrates that our approach effectively immobilizes dsDNA with its strands extending along the surface normal.

Figure 2B shows an image for an array after digestion with *Eco*R1.¹² Importantly, the difference in height between dsDNA addresses and the reference adlayer has decreased to 4.3 ± 0.8 nm (*n*=14). This difference is consistent with the prediction based on the position of the recognition sequence (Figure 1) and agrees with the topographic difference found after the self-assembly of the products produced from off-chip solution digestion. The lack

* To whom correspondence should be addressed.

[†] Microanalytical Instrumentation Center, Ames Laboratory-DOE, and Department of Chemistry.

[‡] Department of Biochemistry, Biophysics, and Molecular Biology.

(1) C6 S-S, Glen Research.

(2) (a) Nuzzo, R. G.; Zegarski, B. R.; Dubois, L. H. *J. Am. Chem. Soc.* **1987**, *109*, 733–740. (b) Biebuyck, H. A.; Whitesides, G. M. *Langmuir* **1993**, *9*, 1766–70.

(3) 5'-Fluorescein phosphoramidite, 6-FAM, Glen Research.

(4) (a) Jones, V. W.; Kenseth, J. R.; Porter, M. D.; Mosher, C. L.; Henderson, E. *Anal. Chem.* **1998**, *70*, 1233–1241. (b) O'Brien, J. C.; Jones, V. W.; Porter, M. D.; Mosher, C. L.; Henderson, E. *Anal. Chem.* **2000**, *72*, 703–710.

(5) (a) Herne, T. M.; Tarlov, M. J. *J. Am. Chem. Soc.* **1997**, *119*, 8916–8920. (b) Peterlinz, K. A.; Georgiadis, R. M.; Herne, T. M.; Tarlov, M. J. *J. Am. Chem. Soc.* **1997**, *119*, 3401–3402.

(6) Lewis, M.; Tarlov, M.; Carron, K. *J. Am. Chem. Soc.* **1995**, *117*, 9574–9575.

(7) Oligonucleotides were exposed to an array formed after Step 3 for 2 h in 1 M THAM (tris(hydroxymethyl)aminomethane) (pH 7.4).

(8) Nuzzo, R. G.; Fusco, F. A.; Allara, D. L. *J. Am. Chem. Soc.* **1987**, *109*, 2358–2368.

(9) Arrays created after Step 4 were exposed to 10 μM MCH (Fluka) (1 M THAM (pH 7.4), 0.1 M MgCl₂) for 1 h.

(10) We estimate the density of dsDNA after MCH treatment to be 60% of its original value. Experiments are underway to more fully characterize oligonucleotide density.

(11) Voet, D.; Voet, J. G. *Biochemistry*; 2nd ed.; John Wiley and Sons: New York, 1995; p. 853.

(12) 5 μL of *Eco*R1 (12 Units/μL, Promega) was diluted to 50 μL with enzyme reaction buffer (90 mM THAM (pH 7.4), 10 mM MgCl₂, and 50 mM NaCl) and placed on the array. Arrays were incubated in a dark, humid environment for 20 h at room temperature. Samples were then rinsed with deionized water and dried with argon. Next, 30 μL of 1 M THAM (pH 7.4) was placed on the array for 1 h at room temperature. Samples were again rinsed with deionized water and dried with argon prior to imaging.

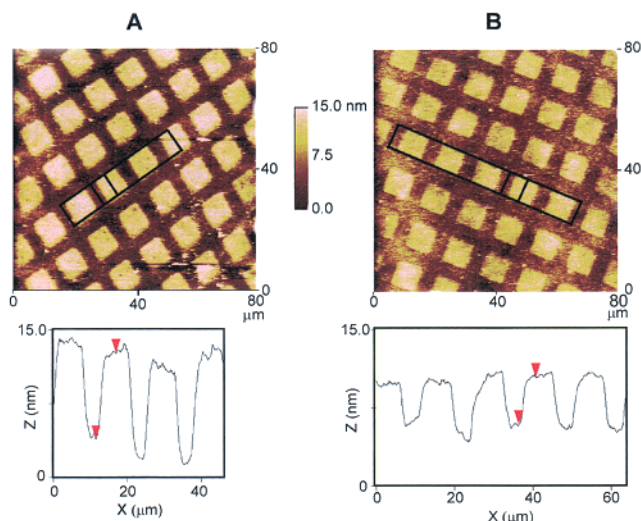


Figure 2. In situ AFM topographic images ($80\ \mu\text{m} \times 80\ \mu\text{m}$) of a dsDNA microarray containing the recognition sequence specific for *EcoR1*. The images were collected before (A) and after (B) digestion with *EcoR1*. The cross-sectional contours below each image reflect the average of the individual scan lines contained in the area of a single row of the array. The in situ images were obtained in 10 mM THAM (pH 7.4) at a scan rate of 1 Hz.

of a detectable optical signal from the fluorescein tag after on-chip digestion also confirms enzymatic cleavage of the target sequence.¹³ We note that digestions of microarrays with *EcoR1* prior to exchange with MCH proved unsuccessful. This finding argues that duplex density is critical for enzymatic access to the recognition sequence.

Figure 3 presents images acquired for an array comprised of double-stranded 26-mers containing the recognition sequence specific for the restriction enzyme *HaeIII*. The heights before ($8.9\ \text{nm} \pm 1.5\ \text{nm}$ ($n=5$)) and after ($8.3\ \text{nm} \pm 1.4\ \text{nm}$ ($n=5$)) exposure to *EcoR1* are effectively indistinguishable. There was also no detectable change in the intensity of the fluorescence pattern.¹³ Both sets of data are diagnostic of the absence of the sequence specific for *EcoR1*, confirming that the observed height decrease in Figure 2 is a direct consequence of the enzymatic cleavage of the specific recognition sequence for *EcoR1*.

Our results show that self-assembled dsDNA microarrays can be readily fabricated and used to screen protein:dsDNA interactions using the topographic imaging capabilities of AFM. As such, our approach to dsDNA microarray construction has several noteworthy attributes with respect to earlier work.¹⁴ First, array fabrication is completely self-assembling in nature (i.e., does not require the use of coupling agents) and is therefore readily

(13) O'Brien, J. C.; Stickney, J. T.; Porter, M. D., manuscript in preparation.

(14) Bulyk, M. L.; Gentalen, E.; Lockhart, D. J.; Church, G. M. *Nat. Biotechnol.* **1999**, *17*, 573–577.

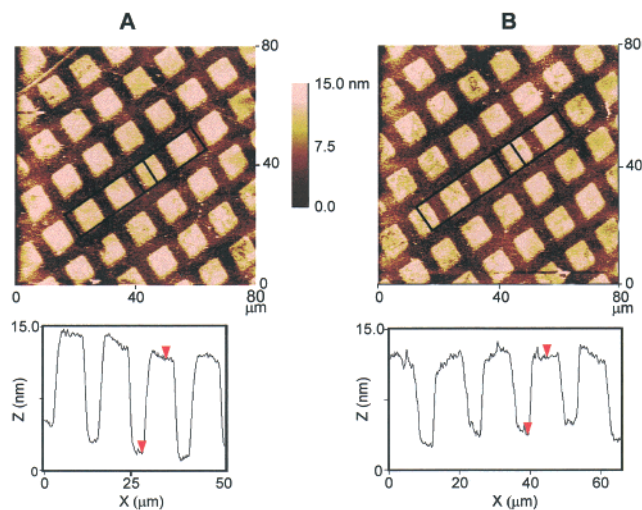


Figure 3. In situ AFM topographic images ($80\ \mu\text{m} \times 80\ \mu\text{m}$) of a dsDNA microarray containing the recognition sequence specific (in bold) for *HaeIII* (5'-GGG AAA GGG AGG CCC AAA GGG AAA GG-3'). The images were collected before (A) and after (B) digestion with *EcoR1*. See Figure 2 caption for further details.

amenable to mass production. Second, our double-stranded oligonucleotide sequences are prepared off-chip by using conventional phosphoramidite chemistry and, as a consequence, potentially have higher fidelities than those synthesized on-chip using light-directed chemistries.^{15,16} The use of AFM also potentially increases the amount of information obtained from screening by extending the conventional two-dimensional read-out of fluorescence imaging to three dimensions. By quantifying the topographic data, it may be possible to determine whether cleavage is highly specific (i.e., targets a specific recognition sequence) or nonspecific (i.e., exhibits star activity). Topographic increases, on the other hand, could be used to discriminate against nonspecific adsorption. Experiments that explore issues of array density, digestion time minimization, and the fabrication of smaller, uniquely modified addresses, are currently underway.

Acknowledgment. We thank J. Harnisch for synthesizing the fluorinated alkanethiol and J.R. Kenseth for helpful discussion. This work was supported in part by the National Science Foundation, the Microanalytical Instrumentation Center, and the Office of Basic Energy Science, Chemical Sciences Division of the U.S. Department of Energy. The Ames Laboratory is operated for the U.S. Department of Energy by Iowa State University under Contract W-7405-eng-82.

JA000411F

(15) (a) Fodor, S. P. A.; Read, J. L.; Pirrung, M. C.; Stryer, L.; Lu, A. T.; Solas, D. *Science* **1991**, *251*, 767–773. (b) McGall, G. H.; Barone, A. D.; Diggelmann, M.; Fodor, S. P. A.; Gentalen, E.; Ngo, N. *J. Am. Chem. Soc.* **1997**, *119*, 5081–5090.

(16) Pease, A. C.; Solas, D.; Sullivan, E. J.; Cronin, M. T.; Holmes, C. P.; Fodor, S. P. A. *Proc. Natl. Acad. Sci. U.S.A.* **1994**, *91*, 5022–5026.